Supplementary Materials

Iron regulates the quiescence of naïve CD4 T cells by controlling mitochondria and cellular metabolism

Authors: Ajay Kumar[a1,2], Chenxian Ye[a,1], Afia Nkansah[a,b], Thomas Decoville[a], Garrett M. Fogo[c], Peter Sajjakulnukit[d], Mack B. Reynolds[a], Li Zhang[d], Osbourne Quaye[b], Young-Ah Seo[f], Thomas H. Sanderson[c,g], Costas A. Lyssiotis[e,g,h], and Cheong-Hee Chang[a,2,3]

A.K. and C.Y. are co-first authors.

[2.] A.K. and C-H.C. are co-senior authors.

[3.] C-H.C. is the lead contact.

This PDF file includes Supplemental text and Figures S1-S6.

Corresponding author: Cheong-Hee Chang heechang@umich.edu

Supplementary text:

Methods

Mice

Male and female C57BL/6 mice ranging in age from 8-12 weeks were either bred in-house or purchased from Jackson Laboratories. FLVCR1-floxed mice were from Dr. Janis Abkowitz (U. of Washington). CD4 Cre and OT-II mice were purchased from the Jackson Laboratories. Mice were housed in specific pathogen-free conditions. All animal experiments were performed in accordance with the Institutional Animal Care and Use Committee of the University of Michigan.

Cell isolation, culture, and proliferation

CD4 T cells were enriched using a negative selection kit according to the manufacturer's instructions (StemCell). Naïve CD4 T cells were sorted. T cells were activated with plate-bound anti-CD3 (5 μg/ml) and soluble anti-CD28 (1 μg/mL) antibodies (eBioscience) for an indicated time in RPMI 1640 medium supplemented with 10% FBS, 2 mM glutamine, and penicillin/streptomycin at 37°C. For OT-II mice, enriched naïve CD4 T cells were stimulated with Ova-peptide (100 μg/ml) (Sigma Aldrich) in the presence of dendritic cells with a ratio of 1:5 of dendritic cells and CD4 T cells for an indicated time in RPMI 1640 medium supplemented with 10% FBS, 2 mM glutamine, and penicillin/streptomycin at 37°C. 50 units of recombinant IL-2 (PeproTech) was used for all IL-2 supplementation experiments. For cell proliferation, CD4 T cells were labeled with CellTrace^{TM} Violet (CTV) (5 μM) (Invitrogen) in 1X PBS containing 0.1% BSA for 20 min at 37°C. To determine the effect of glycolysis, KO CD4 T cells were treated with sodium-lactate (40 mM) and to study the effect of glutamine metabolism using αKG supplementation assays, cells were treated with dimethyl-2-oxoglutarate (DMaKG) (Sigma Aldrich) at a 3 mM concentration.

Flow cytometry assays

The fluorescently-conjugated antibodies used for surface and intracellular staining in the presence of anti-FcγR mAb (2.4G2) were: anti-mouse TCR-β (H57-597) Pacific Blue/APC, anti-mouse CD4 (GK1.5) APC-Cy7, anti-mouse CD8 (53-6.7) PE-Cy7, anti-mouse CD71 (R17217) FITC/PerCP-Cy5.5, anti-mouse CD25 (PC61.5) PerCP-Cy5.5/PE-Cy7, anti-mouse ICAM-1 (3E2) PE, anti-mouse CD69 (H1.2F3) PE-Cy7, and anti-mouse IL-2 (JES6-5H4) PE (all from eBioscience).

For Fpn staining, fixed cells were incubated with a metal transporter protein antibody (rabbit anti-mouse MTP1/IREG1/Ferroprotein, Fpn) (Alpha Diagnostic) in flow cytometry buffer. Ferritin expression was measured by anti-mouse ferritin (EPR3004Y) (Abcam) staining in permeabilization buffer after fixation. To analyze STAT5 phosphorylation, cells were fixed in 80% methanol and stained with rabbit anti-mouse pSTAT5 (Tyr694) (Cell Signaling) antibody. In all staining, AF488-conjugated anti-rabbit secondary antibody (Invitrogen) was used. For intracellular cytokine expression, stimulated CD4 T cells were re-stimulated with 50 ng/mL of PMA (Sigma Aldrich) and 1.5 μM ionomycin (Sigma Aldrich) in the presence of 3 μM monensin for 4 h, followed by intracellular cytokine staining (BD Biosciences). CD98 expression was measured by flow cytometry using the CD98 (RL388) antibody. For intracellular staining of phosphorylated ribosomal protein S6 ($pS6^{Ser235/236}$) (Cell Signaling), $pDRP1^{ser616}$ (Cell Signaling), mitoNEET (CISD1) (Proteintech) and O-GlcNAc (BD Biosciences), cells were permeabilized using 90% methanol. Cells were then incubated with pS6 antibody for 1 h. To examine HBP, cells were stained with the O-GlcNAc antibody and L-PHA (10 μg/ml, Invitrogen) for 30 min at RT in the dark in cytoplasmic permeabilization buffer (BD Biosciences). Dead cells were excluded from the analysis based on the Live/dead Fixable Aqua or Yellow stain (1 μg/mL) (Invitrogen) signal. Cells were acquired on a FACS Canto II or Fortessa (BD Bioscience) and data was analyzed using FlowJo (TreeStar software ver. 10.5). RPMI 1640 media supplemented with 10% dialyzed serum (Sigma-Aldrich).

To measure GSH, cells were stained using an intracellular glutathione detection assay kit (Abcam). Glucose uptake was measured by 2-NBDG (NC0292035) (Invitrogen) in glucose-free

BrdU incorporation

Six-week-old KO and WT littermate mice were injected twice (every 6 hours) intraperitoneally with BrdU (0.5 mg/mouse) (Sigma-Aldrich) in 0.3 ml PBS. PBS injected mice were included as controls. After 18 hrs post-injection, animals were euthanized, and single cell suspensions were prepared from spleens as described earlier. Cells were stained for BrdU incorporation using the BrdU flow kit (BD bioscience) following surface staining, as per the manufacturer's protocol.

Total iron analysis

Sorted naive CD4 T cells were split into replicates containing 1 x 10^6 live cells each and spun down. After removing the supernatant, iron levels were determined by inductively coupled plasma mass spectrometry (ICP-MS) as described previously (1).

Labile iron pool (LIP)

To measure LIP, cells were stained with Calcein-acetomethoxy (Calcein-AM) dye (0.02 μM) (Thermo Fisher) for 10 min at 37°C and analyzed by flow cytometry. LIP was calculated based on the ratio of Calcein MFI in control vs. test samples.

Lipid Peroxidation Assay

A total of 3 x 10^6 splenocytes were stained with a 0.5X Lipid Peroxidation Sensor (Abcam) for 30 min at 37°C according to the manufacturer's instructions. The assay uses a sensitive ratiometric lipid peroxidation sensor, whose fluorescence shifts from red to green in response to lipid peroxidation by ROS in cells, allowing ratiometric (FITC/PE) detection of lipid peroxidation. Cells were then stained with

surface markers in the presence of anti-FcγR mAb (2.4G2) and analyzed by flow cytometry. To inhibit ferroptosis, cells were treated with Ferrostatin-1 (10μM) (Sigma Aldrich).

qPCR assay

Total RNA was isolated from both unstimulated and stimulated naïve CD4 T cells using the RNeasy Plus mini kit (Qiagen) according to the manufacturer's instructions. cDNA was synthesized and qPCR was performed using SYBR Green with Applied Biosystem's 7500HT Sequence Detection System. Fold changes were calculated from ΔCt values using the ΔΔCt method. Expression of target genes was normalized to β-actin.

Glutamine/glutamate and αKG assays

CellTiter-Glo® Luminescent Cell Viability reagent (Promega) was used for ATP measurement. Intracellular glutamate levels were measured using the Glutamine/Glutamate-Glo™ Assay kit (Promega). αKG was measured using a colorimetric assay kit (Sigma Aldrich). All kits were used according to the manufacturer's instructions.

ELISA

Supernatants were collected and ELISA assays were done in conjunction with the University of Michigan ELISA core.

Mitochondrial function

Mitochondrial potential, mitochondrial mass, and mitochondrial ROS (mtROS) were measured using tetramethylrhodamine methyl ester perchlorate (TMRM) (60 nM) (Invitrogen), MitoTrackerTM green (30 nM) (Invitrogen), and MitoSOX (2.5 μM) (Invitrogen), respectively. To measure mitochondrial iron, cells were stained using MitoFerrogreen (5 μM). All these stainings were done by incubating cells for 30 min at 37˚C in RPMI 1640 complete media Cells were then analyzed by flow cytometry.

Cell Microscopy

CD4 T cells were plated onto glass coverslips coated with poly-D-lysine. Cells were washed with PBS and fixed with 4% paraformaldehyde for 15 min at 37°C. Fixed cells were blocked and permeabilized with 5% goat serum (Sigma Aldrich) and 0.3% Triton-X100 (Acros Organics) for 60min. Anti-ATPB (Abcam, ab14730. 1:1000) in 1% BSA (Sigma Aldrich) and 0.3% Triton-X100 was applied to coverslips overnight at 4°C. Coverslips were washed three times with PBS and incubated with Anti-Mouse Alexa Fluor 488 (Invitrogen, A11029, 1:200) in 1% BSA and 0.3% Triton-X100. Coverslips were washed three times with PBS and moused on glass slides with Fluorosheild with DAPI (Sigma Alrdrich, F6057). Duplicate coverslips were used for each experimental replicate.

Cells were imaged on a Zeiss Axio Observer Z1 inverted microscope with LED illumination and 63X oil objective. Images were acquired as z-stacks with 0.24μm z-step to capture entire mitochondrial network. A total of 15-25 images were acquired per experimental replicate containing 2-5 cells per image. Z-stacks were exported as individual frames in TIFF format for post-processing. Analysis of 3D mitochondrial morphology was adapted from previous work (2). Image processing was performed in FIJI. Background fluorescence was removed using a rolling ball radius of 10 pixels. Mitochondria were segmented into binary objects using the Trainable Weka Segmentation plug-in, with a random forest classifier trained against ATPB-positive signal. Segmented images were converted to 8-bit binary and 3D objects were reconstructed using connected components labeling from the MorphoLibJ plug-in library. Stacks were imported into the 3D object manager. Size and geometric measures were obtained for each discrete mitochondrial object. 3D reconstructions were visualized in MeshLab.

Metabolic Seahorse assay

Sorted naïve CD4 T cells from WT and KO mice were stimulated with anti-CD3 and anti-CD28. On one day after stimulation, freshly sorted cells were prepared to use as day 0 samples together with stimulated (day 1) CD4 T cells from WT and KO mice. Live cells were counted and equally deposited in the XF96 well microplate coated with polylysine at a density of 2×10^5 CD4 T cells per well in glucose-free Seahorse media (Sigma Aldrich). The plate was briefly spun to affix the cells to the bottom of the wells. The plate was incubated for 30 min in a non-CO2 incubator. ECAR was measured using glucose (10 mM) (Sigma Aldrich), oligomycin (1 mM, ATP coupler) (Sigma Aldrich), and 2-deoxyglucose (2-DG, 100 mM) (Sigma Aldrich) in seahorse assay medium. OCR was measured using oligomycin (1 mM), FCCP (1.5 mM, Sigma Aldrich), rotenone (1 mM, Sigma Aldrich) and antimycin (1 mM, Sigma Aldrich) in Seahorse assay medium. Both assays were run using a Seahorse XFe96 bioanalyzer (Agilent Technologies).

Metabolite measurements

Cell lysates were prepared from resting and stimulated naive CD4 T cells (5 x 10^5 cells per replicate) by incubating the cells with 80% methanol and following a series of vigorous mixing steps. Cells were spun down at maximum speed for 10 min at 4°C to remove membranous debris, and the lysate was collected for drying using a SpeedVac. Following drying, the lysate was reconstituted using 50/50 methanol/water followed by mass spectrometry-based metabolomics analysis.

A Targeted metabolomics analysis of measured MS/MS spectra with a reference library of 230 standard metabolites was performed using the Agilent Masshunter Workstation Software LC/MS Data Acquisition for 6400 Series Triple Quadrupole MS with Version B.08.02. The LC-MS/MS dynamic multiple reaction monitoring (dMRM) method for detection of 220 metabolites based on MS/MS spectra, retention time (RT) windows, and explicit RTs and was developed by Agilent using 220 individual metabolite standards. An additional 10 metabolites were added to the acquisition method using an identical chromograph method with compound standards.

0.07 min. peak width was used in dMRM scans with an acquisition time of 24 min. Significantly changed metabolites between WT and KO CD4 T cells were determined by comparing the median-centered peak areas with unpaired t tests and filtering of $P < 0.1$ and absolute value of log2 (fold change) > 0.5.

Metabolomics Analysis of U-$^{13}C_6$-Glucose.

For stable isotope analyses, 3×10^5 unstimulated and stimulated, enriched CD4 T cells from WT and FLVCR1 KO mice were incubated in the presence of U-$^{13}C_6$-glucose (15 mM; Sigma Aldrich) and glutamine (2 mM) in glucose-free media containing 10% dialyzed serum for one day at 37°C. Equal number of live WT and FLVCR1 KO CD4 T cells were washed with PBS. After centrifugation, 80% ice cold chilled methanol was added and incubated -80°C for 10 min. The result mixture was centrifuged, and the supernatant was collected and stored at -80°C. Supernatants were dried by speedvac, and the pellets were resuspended in 50uL 50% methanol and water. Metabolomics sample and data analysis were performed following previously published protocols (3).

Statistical analysis

All graphs were prepared using Prism software (Prism version 9; Graphpad Software, San Diego, CA). For comparison among multiple groups, the data was analyzed using a one-way ANOVA with a multi-comparison post-hoc test. For comparison between the two groups, unpaired Student T-tests were used. $P < 0.05$ was considered statistically significant.

References

1. Yarosz et al. Activation-Induced Iron Flux Controls CD4 T Cell Proliferation by Promoting Proper IL-2R Signaling and Mitochondrial Function. J Immunol, 2020

2. Fogo et al. Machine learning-based classification of mitochondrial morphology in primary neurons and brain. Sci Rep **11**, 5133 (2021).

3. Nwosu, et al. Uridine-derived ribose fuels glucose-restricted pancreatic cancer. Nature. 2023

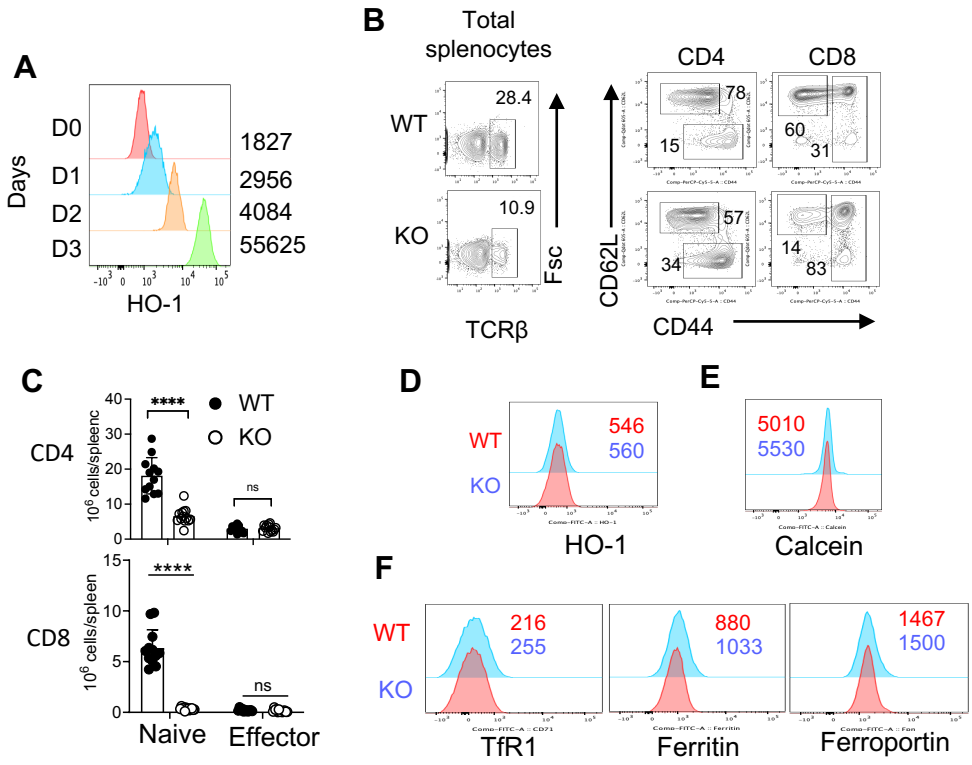

SI Appendix

Fig. S1. Increased intracellular iron in FLVCR1 KO naïve CD4 T cells. (*A*) Enriched naïve CD4 T cells from C57BL/6 mice were activated with anti-CD3 and anti-CD28 as described in the Materials and Methods. The representative histograms show HO-1 expression overtime. (*B*) The representative dot plots show the distribution of total T cells (left panel) and the distribution of naïve and effector CD4 and CD8 T cells from WT and KO mice (right panel). (*C*) The graphs show the total numbers of splenic naïve and effector CD4 (upper panel) and CD8 (lower panel) T cells. (*D*) The representative histograms show the HO-1 expression in WT and KO naïve CD4 T cells. (*E*) The representative histograms show the Calcein signal in WT and KO naïve CD4 T cells. (*F*) The representative histograms show TfR1 (n=4), ferritin (n=6), and Fpn (n=6) in naïve CD4 T cells analyzed from the total splenocytes of WT and KO mice. The data are the cumulative result of at least three independent experiments. Error bars represent the mean ± SEM. ****p<0.0001, ns: not significant.

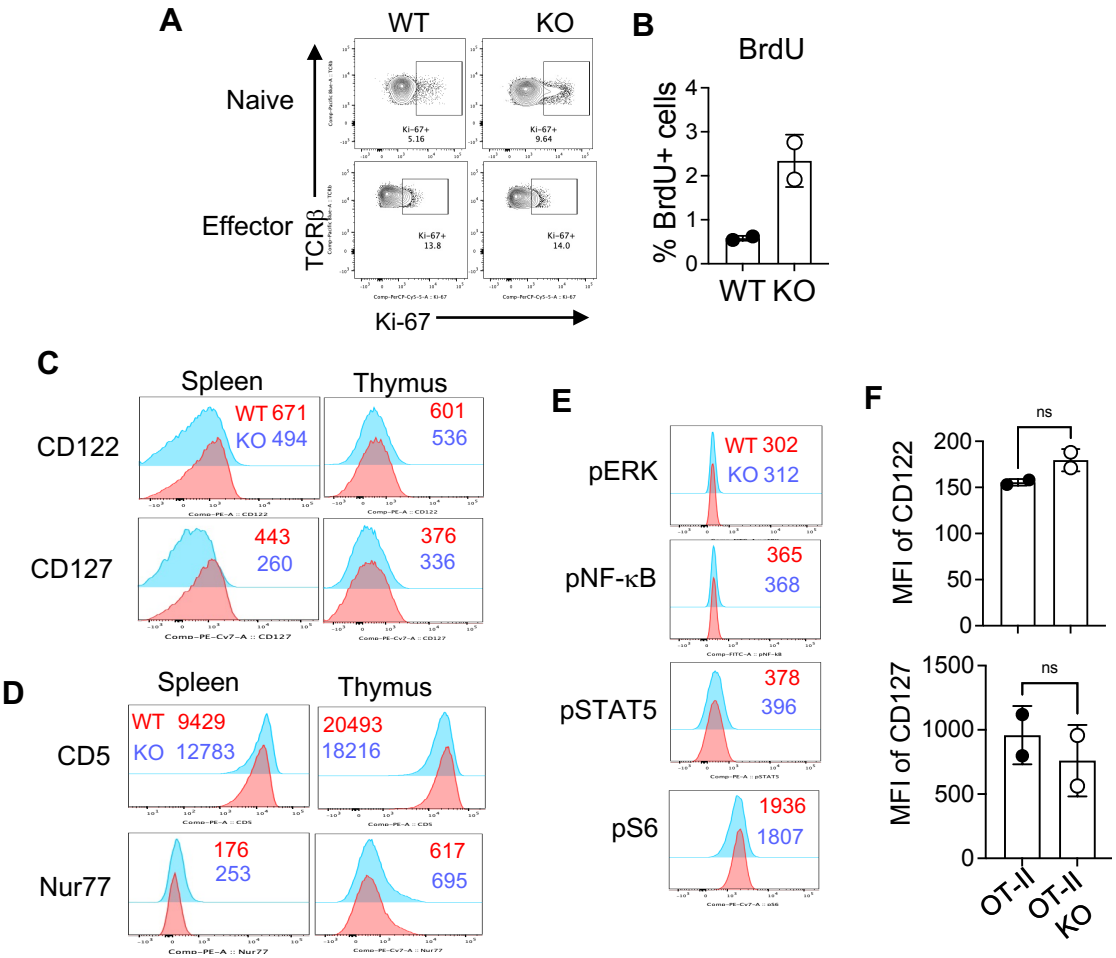

Fig. S2. FLVCR1 deletion alters the homeostasis of naïve CD4 T cells. (*A*) The representative dot plots show percentages of Ki-67$^+$ in naïve (upper panel) and effector (lower panel) CD4 T cells (n=3). (*B*) The graphs show the percentages of BrdU$^+$ naïve CD4 T cells (n=2). (*C*) The representative histograms show the expression of CD122 and CD127 (n=4). (*D*) The representative histograms show expression of CD5 and Nurr77 in splenic naïve CD4 T cells (left panel) and single positive thymic CD4 T cells from WT and KO mice (right panel) (n=3-7). (*E*) Total splenocytes from WT and KO mice were subjected to intracellular staining for signaling molecules as indicated. The representative histograms show expressions of pERK, pNF-ƙB, pSTAT5 and pS6 (n=4) in naïve CD4 T cells. (*F*) Total splenocytes from OT-II and OT-II KO mice were used to assess the expression of CD122 and CD127 on naïve OT-II cells. The graph shows the MFI of CD122 and CD127 (n=2). The data are representative of at least 3 independent experiments. Error bars represent the mean ± SEM. ns: not significant.

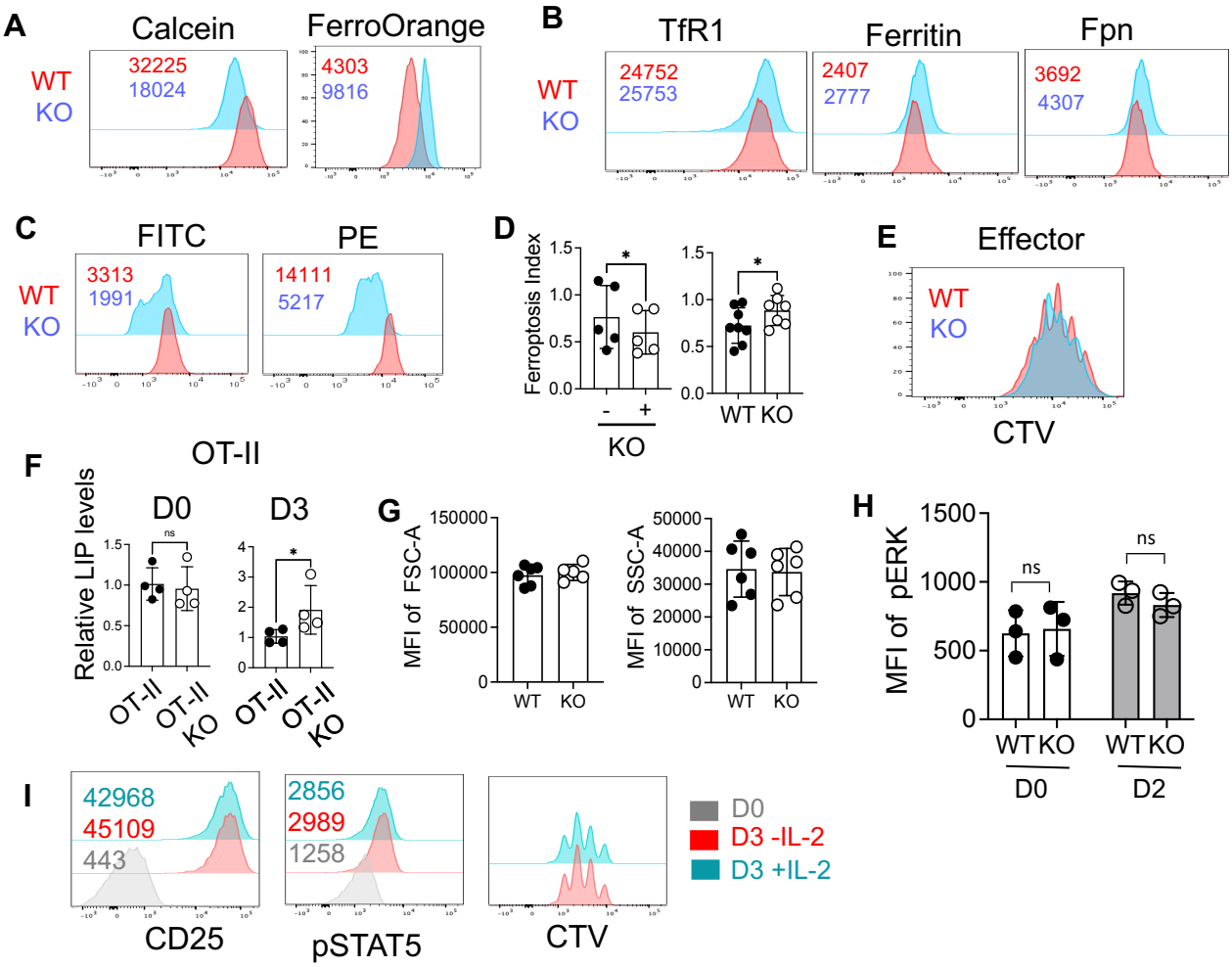

Fig. S3. Iron overload is detrimental to naïve CD4 T cells in response to TCR stimulation. (*A-B*) Sorted naïve CD4 T cells from WT and KO were activated with anti-CD3 and anti-CD28 for 3 days. (*A*) The representative histograms show Calcein and FerroOrange staining 3 days after activation. (n=3-5). (*B*) The representative histograms show the expression of TfR1, ferritin, and Fpn in activated CD4 T cells (n=3-5). (*C*) Sorted naïve CD4 T cells from WT and KO were activated for 3 days. Cells were analyzed for lipid peroxidation. Representative histograms show green (FITC) and red (PE) signals in cells after 3 days of activation. (*D*) Sorted naïve CD4 T cells from WT and KO were activated for 3 days in the absence (-) or presence (+) of 10μM Ferrostatin-1 for 3 days. Ferroptosis index of KO cells on the left indicates the ratio of fluorescence intensity of FITC over PE without (-) or with (+) ferrostatin. The comparison of Ferroptosis index between WT and KO shown on the right was calculated ferroptosis index with ferrostatin over without ferrostatin. (n=5-8) (*E*) Sorted effector CD4 T cells from WT and KO were stained with CellTrace Violet (CTV) and then activated. The representative histograms show cell proliferation (n=3). (*F*) Enriched naïve CD4 T cells from OT-II and OT-II KO mice were stimulated with dendritic cells in the presence of 100 mg/ml of Ova protein. CD4 T cells from these mice were compared for LIP levels at day 0 (D0) and day 3 (D3).

Fig. S3 continued

(*G*) Activated CD4 cells from WT and KO mice were analyzed for FSC and SSC (n=6). (*H*) Activated CD4 cells were subjected to intracellular staining of pERK (n=3). (*I*) KO CD4 T cells were activated with and without IL-2 (50U) and analyzed on day3 for CD25, pSTAT5 and cell proliferation using CTV (n=3). Error bars represent the mean ± SEM. *p<0.05, ns: not significant.

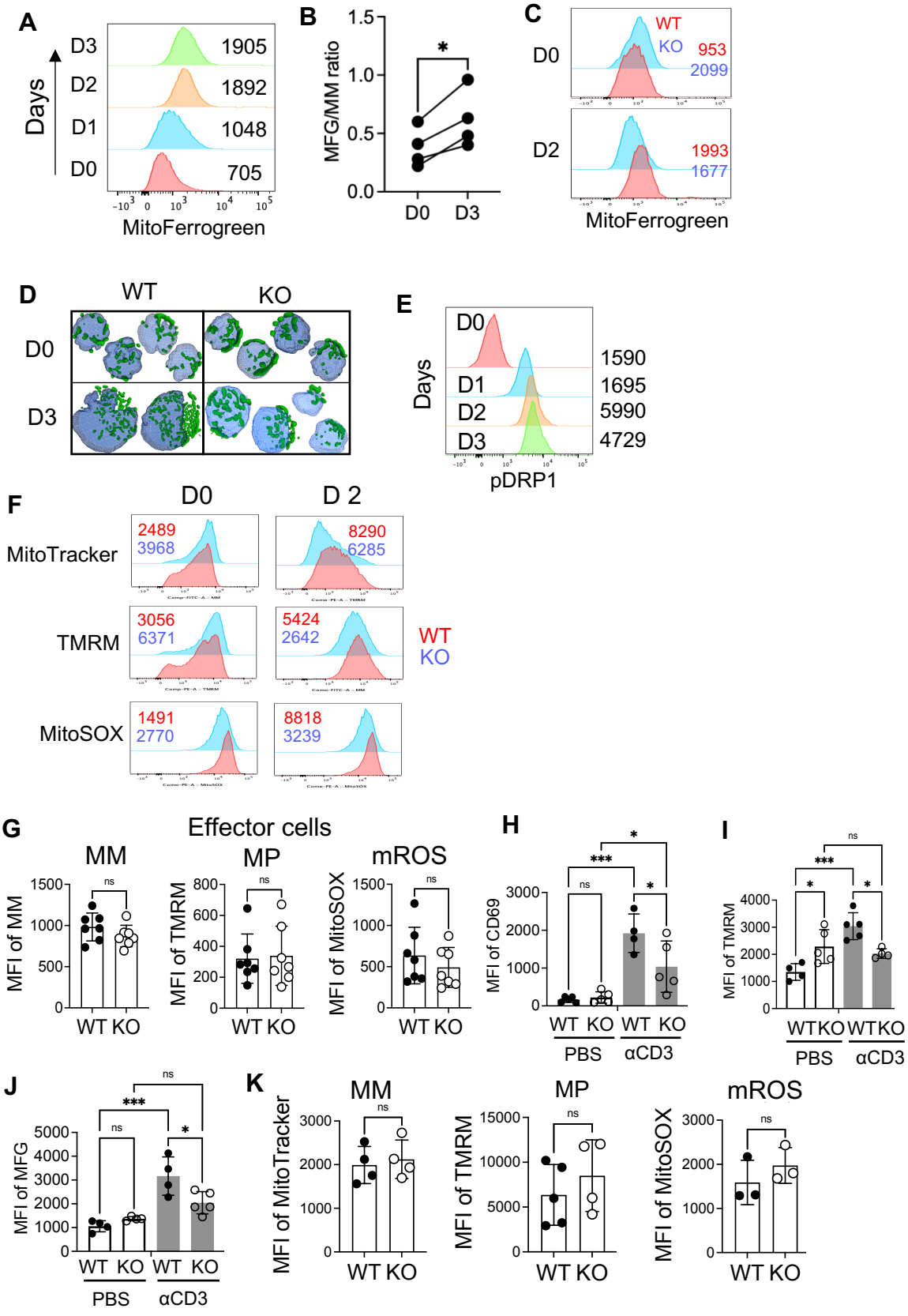
A
Days
D3
D2
D1
D0
1905
1892
1048
705
MitoFerrogreen
B
MFG/MM ratio
1.5
1.0
0.5
0.0
*
D0
D3
C
WT
KO
D0
953
2099
D2
1993
1677
MitoFerrogreen
D
WT
KO
D0
D3
E
Days
D0
D1
D2
D3
1590
1695
5990
4729
pDRP1
F
D0
D 2
MitoTracker
2489
3968
8290
6285
TMRM
3056
6371
5424
2642
WT
KO
MitoSOX
1491
2770
8818
3239
G
Effector cells
MM
MP
mROS
MFI of MM
MFI of TMRM
MFI of MitoSOX
ns
WT KO
H
MFI of CD69
*
***
ns
WT KO WT KO
PBS
αCD3
I
MFI of TMRM
ns
***
*
WTKO WTKO
PBS
αCD3
J
MFI of MFG
ns
***
*
WT KO WT KO
PBS
αCD3
K
MM
MP
mROS
MFI of MitoTracker
MFI of TMRM
MFI of MitoSOX
ns
WT KO

Fig. S4. Mitochondrial fitness and function are compromised in iron-overloaded CD4 T cells. (*A*) Enriched naive CD4 T cells from C57BL/6 mice were activated with anti-CD3 and anti-CD28. Cells were analyzed for mitochondrial iron levels using MitoFerroGreen at the indicated time points. The representative histograms show MitoFerrogreen levels over time (n=4). (*B*) MitoFerroGreen was normalized to mitochondrial mass (n=4). (*C*) Sorted naïve CD4 T cells from WT and FLVCR1 KO were activated for 2 days. Representative histograms show mitochondrial iron in unstimulated (D0) and stimulated (D2) WT and KO CD4 T cells (n=3). (*D*) WT and KO cells without (D0) or with (D3) activation were subjected to ATP synthase (ATPB) staining to mark mitochondria and DAPI for nuclei, followed by visualization via Zeiss Axio Observer with multi-channel LED illumination. Representative images are shown. (*E*) Enriched naïve CD4 T cells from C57BL/6 mice were activated as in (*A*). The representative histogram shows the expression of pDrp1(S616) over time (n=3). (*F-G*) Sorted naïve (*F*) and effector (*G*) CD4 T cells from WT and KO mice were activated with anti-CD3 and anti-CD28 for 2 days. (*F*) Representative histograms show MitoTracker, TMRM and MitoSOX from unstimulated and day 2 stimulated naïve CD4 T cells (n=3). (*G*) Graphs show MFI values of MitoTracker, TMRM and MitoSOX from stimulated effector CD4 T cells. (*H-J*) WT and KO mice were injected intraperitoneally with 200 µl of PBS or anti-CD3 (50 µg/mouse). One day after injection, total splenocytes were used to assess the indicated parameters in naïve ($CD62L^{hi}$, $CD44^{lo}$) CD4 T cells. Summary graphs show MFI of CD69 (*H*), TMRM (**I**) and MitoferroGreen (*J*). (n=4-5). (*K*) Graphs show MFI of MitoTracker green, TMRM, and MitoSOX in CD4 T cells from OT-II and OTII KO mice (n=3-4). The data are representative of at least 3 independent experiments. Error bars represent the mean ± SEM. *p<0.05, **p<0.01, ***p<0.001, ns: not significant.

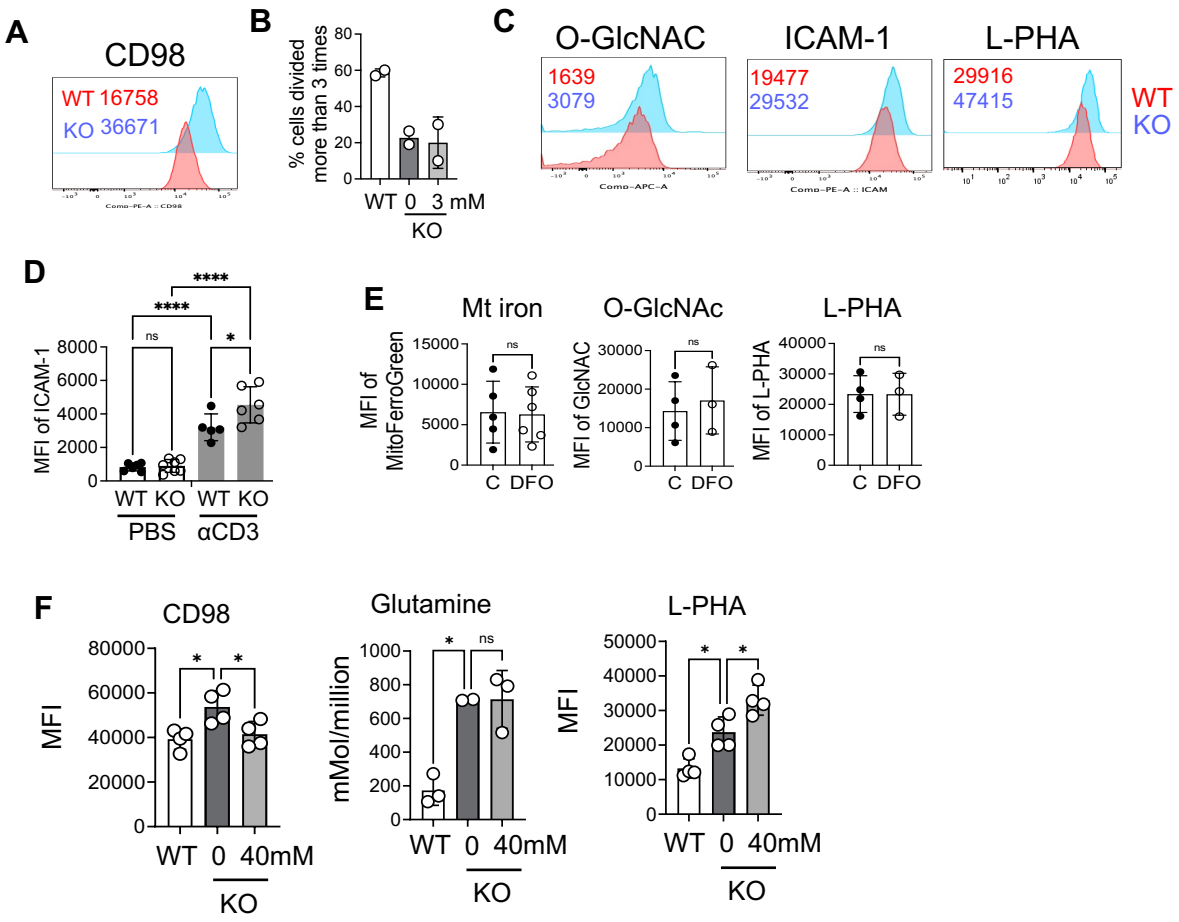

Fig. S5. Iron controls glucose and glutamine metabolism in CD4 T cells. (*A*) Sorted naïve CD4 T cells from WT and KO mice were activated with anti-CD3 and anti-CD28 for 3 days and analyzed for CD98 expression. The representative histograms were shown (n=3) (*B*) Sorted naïve CD4 T cells from WT and KO mice were stimulated for 3 days in the absence or the presence of αKG (3 mM). WT cells did not receive αKG. The graph shows the proliferation of WT and KO CD4 T cells with or without αKG. n=2 (*C*) Cells were prepared as in (*A*). Histograms show O-GlcNAC, ICAM-1 and L-PHA in activated CD4 T cells from WT and KO mice (n=3). (*D*) WT and KO mice were injected intraperitoneally with 200 µl of PBS or anti-CD3 (50 µg/mouse). One day after injection, naïve CD4 T cells in total splenocytes were analyzed for ICAM-1 (n=6). (*E*) Enriched naïve CD4 T cells from C57BL/6 mice were activated without (*C*) or with DFO (4 µM) for 3 days. Cells were analyzed for MitoFerroGreen (mt iron), O-GlcNAc, and L-PHA (n=3-6). (*F*) Sorted naïve CD4 T cells from KO mice were activated for 3 days in the absence or the presence of sodium-lactate (40 mM) and compared for indicated parameters. WT cells did not receive sodium-lactate. N=2-4. The data are representative of at least 3 independent experiments. Error bars represent the mean ± SEM. *p<0.05,****p<0.0001, ns: not significant.

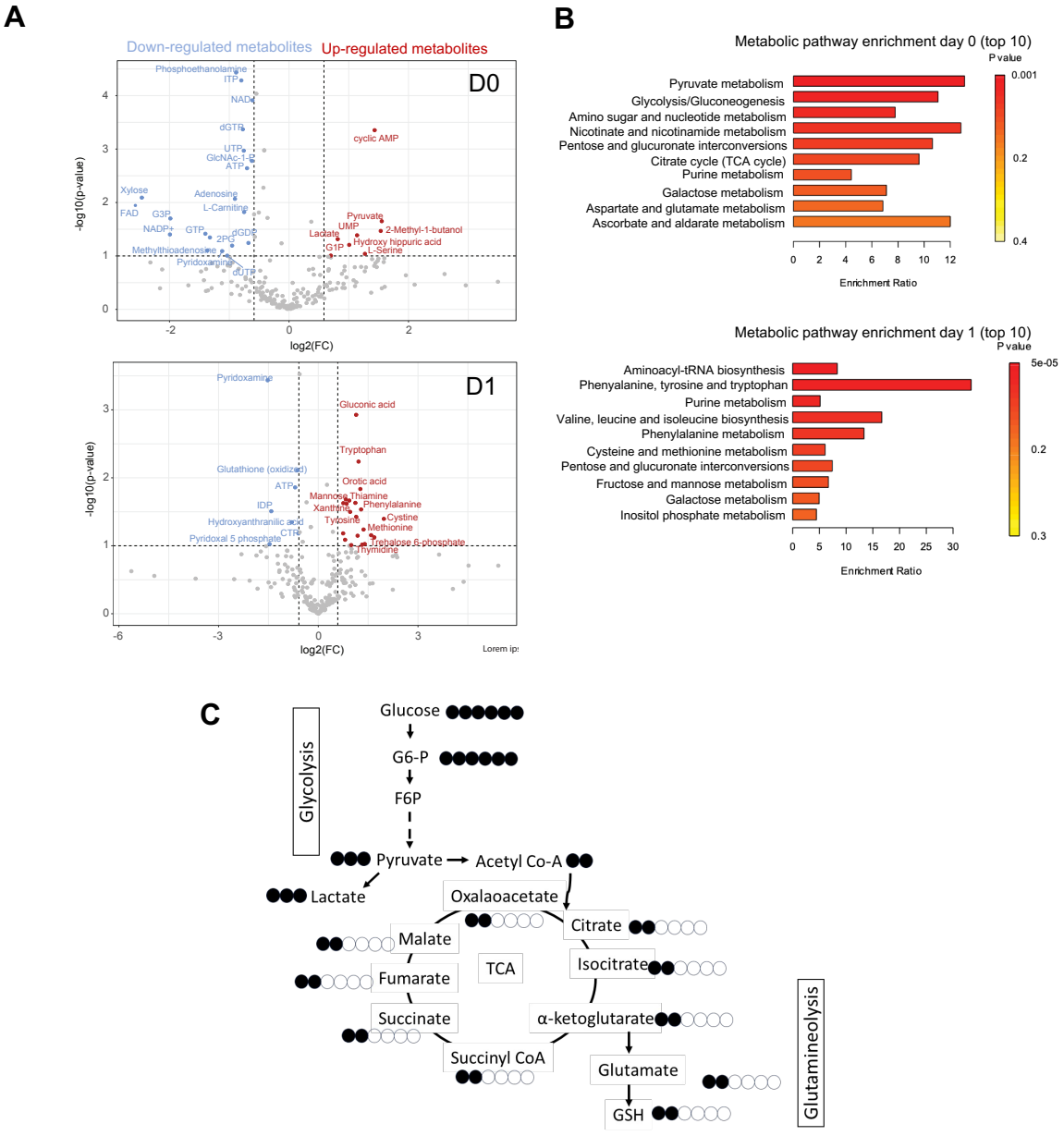

Fig.S6. Iron overload remodels metabolic programming in naïve CD4 T cells. Sorted naïve CD4 T cells from WT and KO mice were activated, and metabolites were extracted from unstimulated (D0) and stimulated cells (D1). Metabolite extracts were subjected to targeted metabolomic analysis using LC-MS/MS with a reference library of 230 metabolites. (*A*) The volcano plot shows the log2 fold change (compared to WT) and log10 (p-value) of metabolites. Red and blue dots denote metabolites that were significantly up- and down-regulated, respectively. (*B*) Pathway enrichment analysis (KEGG) shows distinctly and similarly upregulated pathways in KO compared to WT unstimulated naïve (top) and stimulated CD4 T cells (bottom) (n=3). **(***C***)** A schematic diagram illustrating ^{13}C-Glucose flux. Black and white symbols are ^{13}C-Glucose and regular glucose, respectively.